PHYSICAL REVIEW B VOLUME 56, NUMBER 12 15 SEPTEMBER 1997-II

Metal-insulator transition in layered manganites: $(La_{1-z}Nd_z)_{1.2}Sr_{1.8}Mn_2O_7$

Y. Moritomo, Y. Maruyama, T. Akimoto and A. Nakamura
Center for Integrated Research in Science and Engineering (CIRSE), and Department of Applied Physics, Nagoya University, Nagoya 464-01, Japan

(Received 30 June 1997)

Lattice effects on the anisotropic magnetic and transport properties have been investigated for single crystals of $(La_{1-z}Nd_z)_{1.2}Sr_{1.8}Mn_2O_7$ with a layered structure. The ferromagnetic transition temperature T_C is suppressed from $T_C=130$ K for $z=0.0$ to 80 K for $z=0.2$, and eventually the transition disappears beyond $z=0.4$. From the significant change of the magnetic anisotropy, we have found that the suppression originates from the increasing $d_{3z^2-r^2}$ character in the occupied e_g state due to the Jahn-Teller distortion of the MnO_6 octahedra. Our observations indicate that the effects of chemical substitution are qualitatively different between the cubic and layered doped manganites. [S0163-1829(97)50136-6]

The recent observation of ''colossal'' magnetoresistance[1] (the CMR effect) in the doped manganites has sparked a great amount of effort in understanding the unusual electronic and magnetic properties of these materials. The generic behavior of the ferromagnetic metal (FM) to paramagnetic insulator (PI) transition with CMR near T_C is understood within the framework of double-exchange (DE) theory,[2,3] which includes only the transfer integral t of the e_g electrons and the on-site exchange interaction (Hund's-rule coupling; J_H) between the itinerant e_g electrons and localized t_{2g} spins ($S=3/2$). The magnetoresistance (MR) behavior, especially for $La_{1-x}Sr_xMnO_3$ (Ref. 4) having a large one-electron bandwidth W of the e_g electrons, is well accounted for by the simple DE model.[5] To explain the ''colossal'' value of the MR for the system having small W, e.g., $La_{1-x}Ca_xMnO_3$ (Ref. 6) and $(Nd,Sm)_{1-x}Sr_xMnO_3$,[7] however, we need an additional mechanism for carrier localization above T_C as well as magnetic-field release of the localization. The most intensive mechanism to supplement the DE model is the polaron formation originating from the Jahn-Teller (JT) instability of the MnO_6 octahedra.[8] The most extensively studied manganites $R_{1-x}A_xMnO_3$, where R and A are the trivalent rare-earth and divalent alkaline-earth ions, respectively, have the distorted perovskite structure with three-dimensional networks of the MnO_6 octahedra. In the cubic perovskite manganites, decrease of the averaged ionic radius r_A of the perovskite-A site reduces the one-electron bandwidth W of the e_g band via variation of the Mn-O-Mn bond angle (*chemical pressure* effect[9]). At a fixed nominal hole concentration x, the reduced W suppresses T_C and finally the transition disappears.

In contrast, Moritomo *et al.*[10] have found that the doped manganites $(La,Sr)_3Mn_2O_7$ with a layered structure also show the PI-FM transition accompanying a large MR. In this layered manganite, the MnO_2 sheets are isolated by two La(Sr)O planes, keeping the two-dimensional networks of the MnO_6 octahedra. In addition, the tetragonal crystal field *a priori* lifts degeneracy of the e_g orbitals, and hence the system is free from the dynamical JT effect. Recently, Mitchell *et al.*[11] performed the neutron-diffraction measurements on $La_{1.2}Sr_{1.8}Mn_2O_7$, and found that the MnO_6 octahedra are more severely distorted in the FM state, making a sharp contrast with the cubic manganites.[12] This strongly suggests that we should seek another localization mechanism, at least for the layered materials. Perring *et al.*[13] have performed a neutron-scattering measurement on a single crystal of $La_{1.2}Sr_{1.8}Mn_2O_7$, and observed short-range antiferromagnetic (AF) spin fluctuations above T_C, which can be the alternative origin for the carrier localization.

In this paper, we have investigated lattice effects on the magnetic and transport properties for layered manganites $(La_{1-z}Nd_z)_{1.2}Sr_{1.8}Mn_2O_7$ by partially substituting the smaller Nd^{3+} ions for the larger La^{3+} ions. Reduction of the in-plane Mn-Mn distance with increasing z, which is expected to enhance the t value, suppresses the FM state, and eventually the state disappears beyond $z=0.4$. We have ascribed the suppression of the FM state to variation of the e_g-electron character from the $d_{x^2-y^2}$ to the $d_{3z^2-r^2}$ state and resultant reduction of t. Our observations indicate that the chemical pressure effect is qualitatively different between the cubic and layered doped manganites.

Single crystals of $(La_{1-z}Nd_z)_{1.2}Sr_{1.8}Mn_2O_7$ ($z=0.0$, 0.2, 0.4, 0.6, and 1.0) were grown by the floating-zone method at a feeding speed of 14 mm/h.[10] A stoichiometric mixture of commercial La_2O_3, Nd_2O_3, $SrCO_3$, and Mn_3O_4 powder was ground and calcined two times at 1300 °C for 24 h. The resulting powder was pressed into a rod with a size of 5 mm $\phi\times 60$ mm and sintered at 1350 °C for 48 h. The ingredient could be melted congruently in a flow of air. Large single crystals, typically 4 mm in diameter and 20 mm in length, were obtained with two well-defined facets, which correspond to the crystallographic ab plane. Powder x-ray-diffraction measurements at room temperature and Reitveld analysis[14] indicate that the crystals were single phase without detectable impurities. The crystal symmetry is tetragonal ($I4/mmm$; $Z=2$) over the whole concentration range. Obtained lattice parameters are listed in Table I. The lattice constant a decreases by more than 1% from 3.876 Å for $z=0.0$ to 3.834 Å for $z=1.0$, indicating significant reduction of the in-plane Mn-Mn distance with z. One may notice that the lattice constant c increases with z, which suggests the increasing JT distortion of the MnO_6 octahedra (see also the ratio c/a in the fourth column).

TABLE I. Lattice constants for $(La_{1-z}Nd_z)_{1.2}Sr_{1.8}Mn_2O_7$.

z	a (Å)	c (Å)	c/a
0.0	3.8759(3)	20.1496(9)	5.199
0.2	3.8677(2)	20.1472(7)	5.209
0.4	3.8551(3)	20.1183(8)	5.219
0.6	3.8503(3)	20.1283(8)	5.228
1.0	3.8345(2)	20.1569(9)	5.257

We show in Fig. 1 the temperature dependence of in-plane component ρ_{ab} of resistivity up to ~500 K for single crystals of $(La_{1-z}Nd_z)_{1.2}Sr_{1.8}Mn_2O_7$. For four-probe resistivity measurements, the crystal was cut into a rectangular shape, typically of $3\times2\times1$ mm^3, and electrical contacts were made with a heat-treatment-type silver paint. In the case of $La_{1.2}Sr_{1.8}Mn_2O_7$ ($z=0.0$), a sharp drop of the resistivity by more than two orders of magnitude is observed around $T_C=130$ K (an arrow), reflecting the PI-FM transition.[10] With increasing z, T_C is suppressed to 80 K for $z=0.2$, and eventually the FM phase disappears for $z=0.4$. The resistivity for $z=0.4$ slightly decreases at ~50 K accompanying a prominent thermal hysteresis, which is possibly due to growth of short-range ferromagnetic correlation (*vide infra*). Beyond $z=0.6$, the resistivity remains insulating down to the lowest temperature. Incidentally, a broken curve in Fig. 1 represents out-of-plane component ρ_c of resistivity for $z=0.6$. Anisotropy in resistivity is $\rho_c/\rho_{ab}\approx60$ for $z=0.6$ at 300 K, which is nearly the same value for $La_{1.2}Sr_{1.8}Mn_2O_7$ ($z=0.0$).[10]

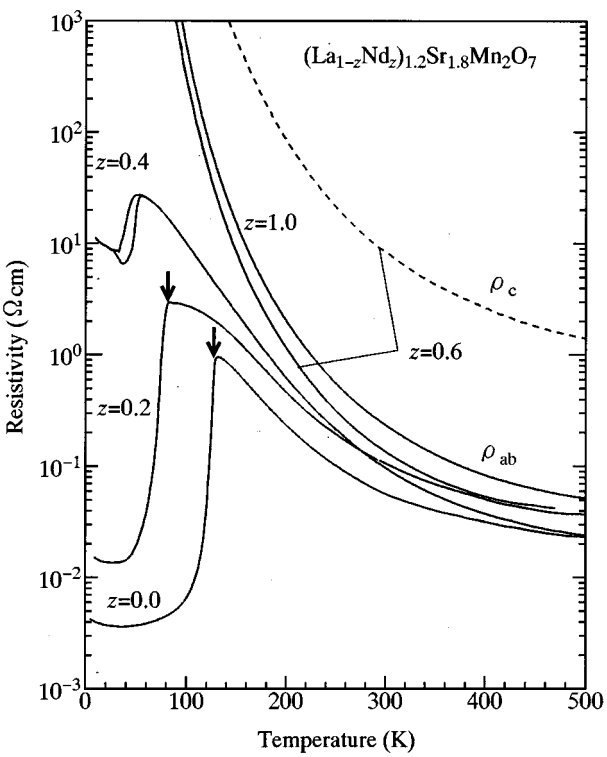

FIG. 1. In-plane component ρ_{ab} of resistivity for single crystals of $(La_{1-z}Nd_z)_{1.2}Sr_{1.8}Mn_2O_7$. A downward arrow indicates the Curie temperature. A broken curve represents the out-of-plane component ρ_c.

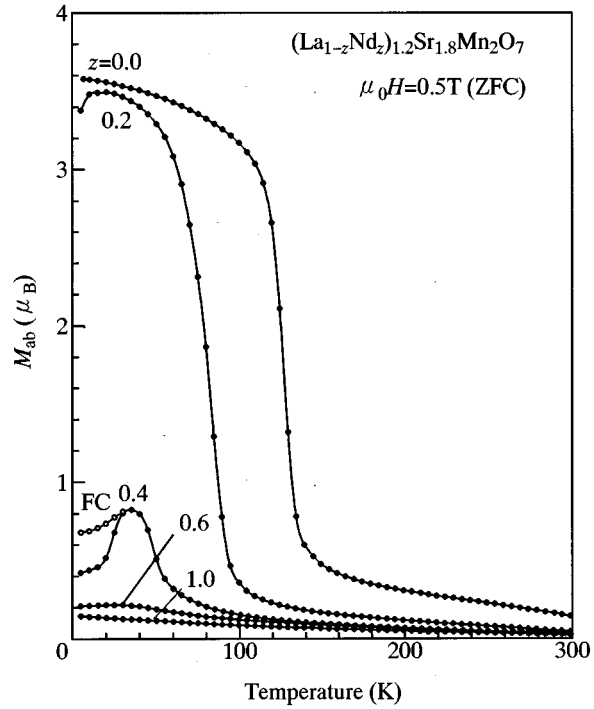

FIG. 2. In-plane components M_{ab} of magnetization for crystals of $(La_{1-z}Nd_z)_{1.2}Sr_{1.8}Mn_2O_7$. M_{ab} was measured under a field of 0.5 T after cooling down to 5 K in zero field (ZFC). Open circles are the data obtained after cooling down to 5 K in the field (FC).

The z-dependent metal-insulator (MI) behavior also shows up in the magnetic properties. Figure 2 shows the in-plane component M_{ab} of magnetization for $(La_{1-z}Nd_z)_{1.2}Sr_{1.8}Mn_2O_7$. M_{ab} was measured under a field

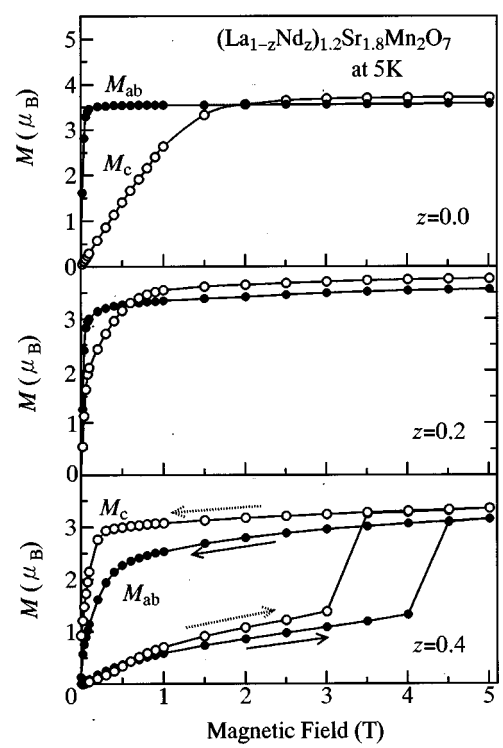

FIG. 3. Magnetization curves for $(La_{1-z}Nd_z)_{1.2}Sr_{1.8}Mn_2O_7$. Applied magnetic field is parallel (M_{ab}; closed circles) and perpendicular (M_c; open circles) to the MnO_2 sheet.

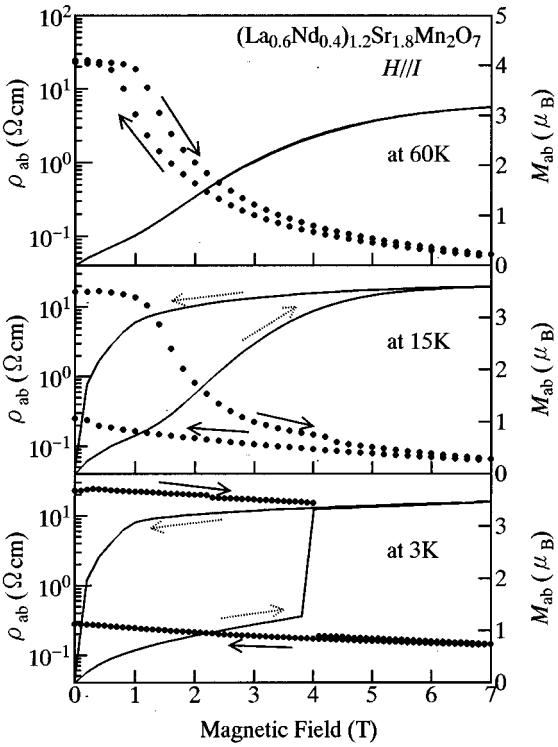

FIG. 4. Magenetoresistance (ρ_{ab}; dots) and magnetization (M_{ab}; solid curve) for $(La_{0.6}Nd_{0.4})_{1.2}Sr_{1.8}Mn_2O_7$ ($z=0.4$). Magnetic field H was applied parallel to the current $I \| ab$.

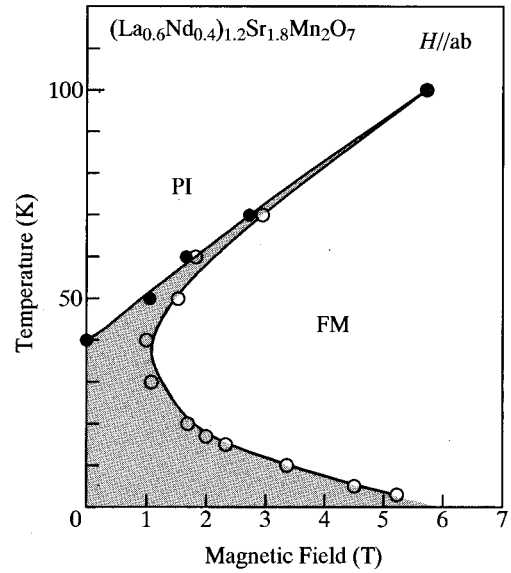

FIG. 5. Magnetic phase diagram for $(La_{0.6}Nd_{0.4})_{1.2}Sr_{1.8}Mn_2O_7$ ($z=0.4$) against an external magnetic field. Open and closed circles represent the upper and lower critical fields, H_{cu} and H_{cl}, respectively. PI and FM stand for paramagnetic insulator and ferromagnetic metal, respectively. The hatched area is the hysteretic region.

of $\mu_0 H=0.5$ T using a superconducting quantum interference device (SQUID) magnetometer. The $M_{ab}-T$ curve for $La_{1.2}Sr_{1.8}Mn_2O_7$ ($z=0.0$) steeply rises below $T_C=130$ K and reaches near the ideal value ($=3.6\ \mu_B$). Magnitude of M_{ab} for $z=0.2$ becomes nearly the same value at low temperature, even though T_C shifts to the low-temperature side ($T_C=80$ K). The $M_{ab}-T$ curve for $z=0.4$ is rather complicated; M_{ab} rises below ~ 50 K and subsequently drops at ~ 40 K. The rise of M_{ab} suggests growth of ferromagnetic clusters, which may cause the observed decrease of resistivity at ~ 50 K (see Fig. 1). On the other hand, reduction of M_{ab} at ~ 40 K is presumably ascribed to a transition to a spin-glass-like state, which corresponds to the gradual increases of ρ_{ab}. Beyond $z=0.6$, the $M_{ab}-T$ curve becomes temperature insensitive.

Now, let us see the lattice effect on the magnetic anisotropy. Figure 3 shows the magnetization curves at 5 K. For $z=0.0$, the magnetization shows a large anisotropy ($M_{ab}/M_c \sim 20$) under a low field of 10 mT, indicating that the easy axis lies on the MnO_2 sheet.[10] The anisotropy M_{ab}/M_c, however, rapidly decreases to ~ 2 for $z=0.2$, and almost vanishes for $z=0.4$. The magnetization curve for $z=0.4$ shows an abrupt jump at $\mu_0 H \approx 4$ T for $H \| ab$ and at $\mu_0 H \approx 3$ T for $H \| c$, indicating a paramagnetic-to-ferromagnetic transition. In the field-induced ferromagnetic phase, the easy axis is along the c direction, making a sharp contrast with the case for $z=0.0$. The change of the easy axis direction perhaps originated as a variation of the e_g-electron character. The magnetization curves for $z=0.6$ and 1.0 (not shown) continue increasing beyond 5 T, showing a paramagnetic behavior.

The suppression of the FM state by increasing z is apparently curious, because one may expect that reduction of the in-plane Mn-Mn distance increases both t and T_C. Such a contradiction is well solved if we consider variation of the e_g-electron character in the following way. Reflecting the layered structure, the degenerated e_g orbitals are split into the $d_{x^2-y^2}$ and $d_{3z^2-r^2}$ states; the former extends along the sheet direction and has large t, while the latter has small t. Recently, Park *et al.*[15] have performed x-ray absorption spectroscopy (XAS) and angle-resolved photoemission spectroscopy (ARPES) on a single crystal of $La_{1.2}Sr_{1.8}Mn_2O_7$ ($z=0.0$), and found that the $d_{x^2-y^2}$ character dominates the occupied e_g state even though the $d_{x^2-y^2}$ state locates slightly above the $d_{3z^2-r^2}$ state. Accordingly, the relatively large t can cause the FM state at low temperatures. With increasing z, however, the MnO_6 octahedra elongate along the c axis (see Table I); at room temperature, the in-plane Mn-O bond length decreases from 1.937 Å for $z=0$ to 1.921 Å for $z=1$, while the averaged out-of-plane bond length increases from 1.968 Å for $z=0$ to 1.987 Å for $z=1$.[11] Such a distortion modifies the crystal field around the e_g state, and further stabilizes the $d_{3z^2-r^2}$ state. Thus, we expect the increasing $d_{3z^2-r^2}$ character in the occupied e_g state, which can explain the observed change of the magnetic anisotropy (see Fig. 3). Resultant reduction of t causes the observed MI phenomenon. This scenario is also supported by the fact that $La_{1.4}Ca_{1.6}Mn_2O_7$ ($x=0.3$),[16] whose lattice constant c ($=19.24$ Å) is much shorter, has higher T_C ($=140$ K) as compared with that for $La_{1.4}Sr_{1.6}Mn_2O_7$ ($T_C=90$ K).

Near the MI phase boundary, an external magnetic field significantly affects the magnetic and transport properties. Shown in Fig. 4 is the magnetic-field effect on ρ_{ab} and M_{ab} for $z=0.4$. At 3 K (the lower panel), the M_{ab} value gradually increases below ≈ 4 T, and discontinuously jumps from ≈ 1.2 to $\approx 3.4\ \mu_B$, accompanying a sudden drop of ρ_{ab} by almost two orders of magnitude. Such a PI-FM transition is

observed even at 60 K (upper panel); ρ_{ab} begins to decrease above $\mu_0 H \approx 1$ T. Note that a similar metamagnetic behavior accompanying a steep drop of ρ_{ab} is also observed above T_C for $La_{1.2}Sr_{1.8}Mn_2O_7$ ($z=0.0$; see Fig. 4 of Ref. 10). The MR behavior for $z=0.0$ can be viewed as a transition from the PI state with short-range AF fluctuation[13] to the FM state, because an external magnetic field suppresses spin fluctuations and releases the carrier localization. Hereafter, we will define the upper and lower critical fields, H_{cu} and H_{cl}, as the corresponding inflection points of the $M_{ab}-T$ curve. We plotted in Fig. 5 the obtained critical fields; open circles are for H_{cu} and closed circles for H_{cl}. A hatched area represents a bistable region where the PI and FM state can coexist. At temperatures above ~ 70 K, the transition exhibits a rather small field hysteresis. The hysteretic region, however, becomes broader when the temperature is lowered; especially, the field-induced FM state remains stable even at zero field below ~ 40 K. According to classical thermodynamics, the first-order phase transition of the metastable state takes place when the potential barrier between the two states becomes comparable with temperature. As a result, reduction of temperature suppresses the transitions between the metastable states.

In conclusion, we have investigated lattice effects on the anisotropic magnetic and transport properties for the doped manganites $(La_{1-z}Nd_z)_{1.2}Sr_{1.8}Mn_2O_7$ with a layered structure. With increasing z, the ferromagnetic metal (FM) state is significantly suppressed, and eventually the transition disappears beyond $z=0.4$. Considering the increasing static distortion of the MnO_6 octahedra and the variation of the magnetic anisotropy, the MI phenomenon is found to be driven by the increasing $d_{3z^2-r^2}$ component of the e_g electrons and resultant reduction of t. In the layered manganites, the character of the e_g electrons can be controlled by application of the chemical pressure, which will lead us to *orbital physics*.

The authors are grateful to J. F. Mitchell, D. Dessau, T. Saito, N. Hamada, and N. Furukawa for fruitful discussions. This work was supported by a Grant-In-Aid for Scientific Research from the Ministry of Education, Science and Culture, Japan and also from Murata Science Foundation and the Research Foundation for Materials Science.

[1] For example, see S. Jin, T. H. Tiefel, M. McCormack, R. Fastnacht, R. Ramesh, and L. H. Chen, Science **264**, 13 (1994).

[2] P. W. Anderson and H. Hasagawa, Phys. Rev. **100**, 675 (1955).

[3] P-G. de Gennes, Phys. Rev. **118**, 141 (1960).

[4] A. Urushibara, Y. Moritomo, T. Arima, A. Asamitsu, G. Kido, and Y. Tokura, Phys. Rev. B **51**, 14 103 (1995); Y. Tokura, A. Urushibara, Y. Moritomo, T. Arima, A. Asamitsu, and G. Kido, J. Phys. Soc. Jpn. **63**, 3931 (1994).

[5] N. Furukawa, J. Phys. Soc. Jpn. **63**, 3214 (1994); **64**, 2734 (1995); **64**, 2754 (1995); **64**, 3164 (1995).

[6] P. Schiffer, A. P. Ramirez, W. Bao, and S.-W. Cheong, Phys. Rev. Lett. **75**, 3336 (1995).

[7] H. Kuwahara, Y. Tomioka, Y. Moritomo, A. Asamitsu, M. Kasai, R. Kumai, and Y. Tokura, Science **272**, 80 (1996).

[8] A. J. Millis, P. B. Littlewood, and B. I. Shraiman, Phys. Rev. Lett. **74**, 5144 (1994); **77**, 175 (1996).

[9] H. Y. Hwang, S-W. Cheong, P. G. Radaelli, M. Marezio, and B. Batlogg, Phys. Rev. Lett. **75**, 914 (1995).

[10] Y. Moritomo, A. Asamitsu, H. Kuwahara, and Y. Tokura, Nature (London) **380**, 141 (1996).

[11] J. M. Mitchell, D. N. Argyriou, J. D. Jorgensen, D. G. Hinks, C. D. Potter, and S. D. Bader, Phys. Rev. B **55**, 63 (1997); J. F. Mitchell, D. N. Argyriou, C. D. Potter, J. D. Jorgensen, D. G. Hinks, and S. D. Bader, Mater. Res. Soc. Symp. Proc. **453**, 343 (1997).

[12] For example, see P. G. Radaelli, M. Marezio, H. Y. Hwang, S-W. Cheong, and B. Batlogg, Phys. Rev. B **54**, 8992 (1996).

[13] T. G. Perring, G. Aeppli, Y. Moritomo, and Y. Tokura, Phys. Rev. Lett. **78**, 3197 (1997).

[14] F. Izumi, in *The Rietveld Method*, edited by R. A. Young (Oxford University Press, Oxford, 1993), Chap. 13; Y.-I. Kim and F. Izumi, J. Ceram. Soc. Jpn. **102**, 401 (1994).

[15] C.-H. Park, D. S. Dessau, T. Saitoh, Z.-X. Shen, Y. Moritomo, and Y. Tokura (unpublished).

[16] H. Asano, J. Hayakawa, and M. Matsui, Appl. Phys. Lett. **70**, 2303 (1997).